2
IONOSPHERE

Darrell F. Strobel and Sushil K. Atreya

Our understanding of Jupiter's ionosphere has been enhanced by the Voyager encounters. Vibrationally excited H_2 ($v \geq 4$) probably played an important role in providing a rapid loss mechanism for protons (the major topside ion) during the Voyager encounter. A straightforward calculation of the Voyager 1 entry electron concentration profile with chemistry and physics adequate to understand the Pioneer radio occultation profiles yields significant differences from the Voyager radio science measurements and suggests that substantial improvements in models may be necessary if the preliminary results of the observations remain unaltered after improved reduction and analysis of the data. It is argued that, although solar EUV radiation probably controlled the ionosphere during the Pioneer observations, particle precipitation as evidenced by strong H_2 airglow emissions on a planetwide basis appears to have played an essential role in both heating the thermosphere and as an ionization source during the Voyager encounters. The main contribution to the Pedersen conductivity in Jupiter's ionosphere occurs in the region where multilayer structure is dominant and accurate reductions of the Voyager radio occultation measurements are not yet available. Theoretical estimates of the integrated Pedersen conductivity are in the range of 0.02–10 mho; the former values are representative of an ionosphere produced by solar EUV radiation and the latter of the auroral ionosphere under intense particle precipitation.

2.1. Introduction

The original interest in an ionosphere on Jupiter was generated by the discovery of strong radio-frequency emissions at ~20 MHz that were thought to be plasma frequencies associated with Jupiter's ionosphere [Gardner and Shain, 1958]. A historical summary of developments in our understanding of Jupiter's ionosphere may be found in Strobel [1979]. The ionosphere of Jupiter provides a means to couple the magnetosphere to the atmosphere by virtue of its high conductivity and collisional interaction with the neutral atmosphere. The Pioneer and Voyager spacecraft have done much to stimulate interest in Jupiter's ionosphere by providing direct measurements of profiles of electron concentration at selected locations on Jupiter. Detailed measurements of ionospheric structure provide important information on the neutral atmosphere and physical processes that affect its structure in addition to data of purely ionospheric interest. Because a number of reviews on Jupiter's ionosphere have appeared previously [Hunten, 1969; McElroy, 1973; Huntress, 1974; Atreya and Donahue, 1976; Strobel, 1979], this chapter emphasizes the contributions from the Voyager program to our understanding of Jupiter's ionosphere.

2.2. Basic principles

The most fundamental quantities needed to understand the ionosphere are the electron and ion concentrations as a function of altitude, latitude, and, in the case of Jupiter, longitude. They are solutions of the electron continuity equation

$$\frac{\partial n_e}{\partial t} + \nabla \cdot \bar{\phi}_e = P_e - \alpha n_e^2 \tag{2.1}$$

and ion continuity equation

$$\frac{\partial n_i}{\partial t} + \nabla \cdot \overline{\phi}_i = P_i - L_i n_i \tag{2.2}$$

where n is the concentration, $\overline{\phi}$ the flux, P the production rate per unit volume, L the loss rate, and α the recombination rate. The subscripts e and i refer to electrons and ions, respectively. The constraint of electrical neutrality requires $n_e \equiv \Sigma_i n_i$. The only adequately understood sources of electrons and ions are solar extreme ultraviolet (EUV) photoionization of neutral atmospheric species and subsequent ionization by the ejected photoelectrons. Jupiter's ionosphere is peculiar when compared to other planetary ionospheres in that energetic-particle precipitation exhibits distinct longitudinal asymmetry and day–night asymmetry as evidenced by optical signatures obtained in the ultraviolet [Broadfoot et al., 1981]. Appropriate asymmetries in $P_{e,i}$ and hence $n_{e,i}$ are expected. An unfortunate aspect of particle precipitation is that direct measurements are not available and only indirect inferences from optical signatures can be used to estimate source strength and spatial variation of $P_{e,i}$. During the period of the Voyager encounter it appears that, in high magnetic latitudes, particle precipitation was the major source of ionization, atomic hydrogen, and heat for the thermosphere. In contrast, ion chemistry and plasma recombination processes for Jupiter's ionosphere are fairly well understood, as reviewed below.

Redistribution of plasma as represented by the flux divergence terms is not understood for Jupiter with the exception of ambipolar diffusion along magnetic flux tubes. Horizontal wind systems in Jupiter's thermosphere could transport plasma along the flux tubes by ion drag to raise or lower ionospheric layers. Intense heating of auroral regions as observed by Voyager would drive a wind system similar to that modeled by Roble et al. [1979] for the Earth. At midlatitudes, upward plasma drifts of as much as 50 ms^{-1} could be generated by this wind system. Dynamo electric fields and $\mathbf{E} \times \mathbf{B}$ drifts could be as important for vertical transport across the horizontal, equatorial magnetic fields as in the Earth's equatorial ionosphere. Unfortunately the magnitude of these electric fields in Jupiter's dynamo region is not known.

2.3. Ionization sources

From our terrestrial experience, we would expect solar EUV radiation to dominate the production of ionization in the main ionospheric layers of Jupiter in spite of the reduction in solar flux by a factor of 27 relative to Earth. Solar EUV ionization is most relevant for the equatorial ionosphere outside of the Lyman-α bulge region, whereas particle ionization plays a significant role at high latitudes. The major ionizable constituents H_2, He, and H require solar photons shortward of 804, 504, and 912 A (1 A = 10^{-10} m), respectively, to eject an electron. Direct photoionization of H_2 is the major ionization channel. At the time of the Pioneer observations, direct photoionization of H was a negligible source of protons for the ionosphere. The most potent source of H^+ was dissociative photoionization of H_2 [McElroy, 1973] as illustrated in Figure 2.1. The principal reason is that for average solar activity, atomic hydrogen remains a minor constituent ($\sim 10^{-3}$ [H_2]) in the main ionospheric region. However, during Voyager observations the increased Lyman-α albedo implies much greater atomic hydrogen abundances [Yung and Strobel, 1980] and thus enhanced direct photoionization of H [Atreya, Donahue, and Waite, 1979]. Helium, with a greater abundance than H (during the Pioneer encounter), has a large ionization production rate in spite of its high ionization potential (see Fig. 2.1). Photoelectrons

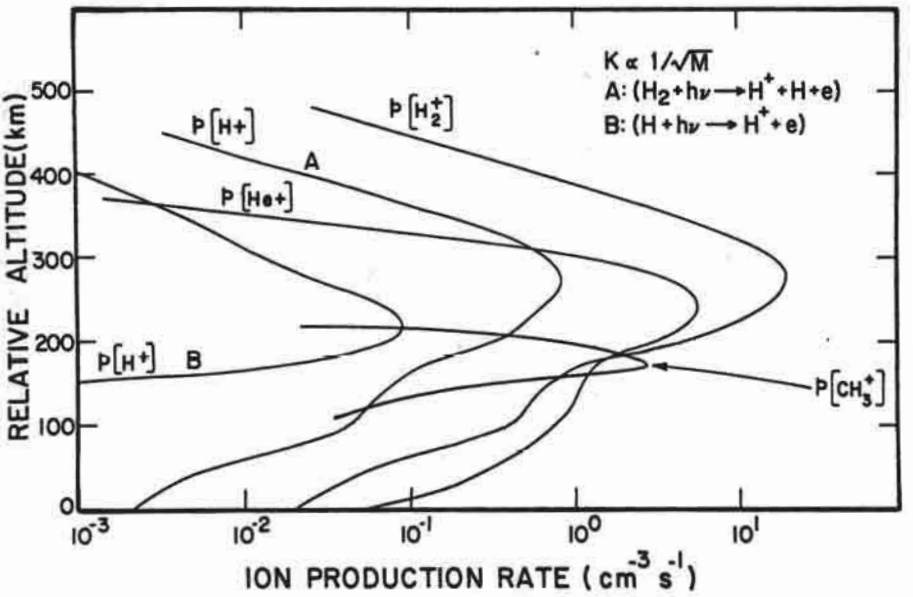

Fig. 2.1. Ion production rates $p(X^+)$ by solar EUV radiation with solar zenith angle of 60° for a model atmosphere with the eddy diffusion coefficient $K \propto [M]^{-1/2}$, where M is the neutral concentration, and equal to 3×10^7 cm^2 s^{-1} at the turbopause appropriate for Pioneer observations. The height scale refers to the altitude above the level at which the atmospheric density is 10^{16} cm^{-3}. Note that the CH_3^+ production rate is based on revised CH_3 densities from Yung and Strobel [1980] (after Atreya and Donahue [1976]).

produced in the ionization process are not an important source of protons according to the analysis of Cravens, Victor, and Dalgarno [1975]. In Jupiter's ionosphere, the CH_3 radical may play a comparable role to that of NO in the Earth's lower ionosphere. With a low ionization potential, it is ionized by absorption of solar Lyman-α and initiates the formation of a low-lying ionization layer [Prasad and Tan, 1974, Fig. 1].

The importance of galactic cosmic rays as an ionization source is enhanced relative to the Earth by the drop in solar radiation intensity with increasing distance from the Sun [Capone et al., 1976, 1977]. Calculation of ion production rates by cosmic ray bombardment of Jupiter is complicated. The most recent computation was by Capone et al. [1979], who obtained a peak ionization rate of ~ 10 cm^{-3} s^{-1} at a magnetic latitude of 60° and neutral concentration of 10^{19} cm^{-3}.

Another potentially important ionization source on Jupiter is neutral atoms and molecules ejected from the Galilean satellites under the intense radiation environment of the extensive Jovian magnetosphere. Under bombardment by keV or MeV particles from the Jovian magnetosphere, material can be sputtered off the surfaces of the Galilean satellites [Matson, Johnson, and Fanale, 1974]. In the case of Io, this process probably results in the formation of an extensive, but incomplete, torus of neutral sodium [R. A. Brown, 1974, Chapter 6]. From the Voyager encounters with Jupiter we know that Io is the site of intense volcanic activity [Morabito et al., 1979], has an SO_2 atmosphere [Pearl et al., 1979], and is the source of S and O ions observed in the Io plasma torus [Bridge et al., 1979a Broadfoot et al., 1979]. Although the details of how and where neutral particles are injected in the torus are uncertain, the ionization of neutrals occurs primarily by electron impact and at a rate of (2–20) $\times 10^{28}$ ion s^{-1} (see

Chap. 3 and 6). The newly created ions are accelerated and swept away by the Jovian magnetic field that rotates more rapidly than the satellites.

Siscoe and Chen [1977] have argued that the major loss of this ionization is radial diffusion by flux tube interchange, which is driven by electric fields associated with winds in Jupiter's ionosphere [Brice and McDonough, 1973; Coroniti, 1974]. Siscoe [1978a] has estimated probabilities for inward radial diffusion from individual satellites. In the case of Io, he estimated 0.52 for low concentrations of torus plasma. From analysis of Voyager data, Richardson et al. [1980] suggest that 0.1 is more appropriate for high concentrations of torus plasma. These inward-diffusing ions are eventually captured by the parent planet, whereas the outward-diffusing ions are lost by interaction with the solar wind. Based on the supply rate of ions to the plasma torus, we estimate that the flux of oxygen and sulfur ions and associated electrons into Jupiter's atmosphere may be as large as 3×10^7 cm^{-2} s^{-1}, which corresponds to a total flux of about 10^{28} s^{-1}. The energy distribution of these entering ions and associated electrons is unknown. The loss of particles into the atmosphere may be asymmetric as discussed below.

In spite of these uncertainties there is considerable evidence for precipitating particles (probably electrons) into Jupiter's equatorial and polar atmospheres from observations of intense H_2 band emission by the Voyager UVS [Sandel et al., 1979, 1980; McConnell, Sandel, and Broadfoot, 1980]. The nightside Lyman-α observed by the Voyager UVS also requires particle precipitation to explain the measured intensity [McConnell, Sandel, and Broadfoot, 1980]. A distinct peculiarity of the equatorial H_2 emissions is that their intensity seems to depend on whether the Sun is shining (Sandel et al., 1979; McConnell, Sandel, and Broadfoot, 1980; Broadfoot et al., 1981). During the day the H_2 Lyman and Werner band intensity was observed to be 2.8 ± 1.0 kR, whereas at night an upper limit of 500 R was obtained [Broadfoot et al., 1981; McConnell, Sandel, and Broadfoot, 1980]. In addition to this day–night asymmetry, there is a pronounced longitudinal asymmetry in the Lyman-α brightness of Jupiter with peak intensity at $\lambda_{III} \sim 80$–$120°$ W, and latitude ~ 8–$12°$ N [Sandel, Broadfoot, and Strobel, 1980; Clarke et al., 1980; Dessler, Sandel, and Atreya, 1981]. Although the Lyman-α bulge is a manifestation of resonance scattering of solar Lyman-α from an enhanced H column density region above the absorbing CH_4 layer [Sandel, Broadfoot, and Strobel, 1980], the atomic hydrogen bulge is created by convecting, corotating magnetospheric electrons (~ 100 keV and ~ 1 erg cm^{-2} s^{-1}) precipitating preferentially in the longitude and latitude region of the Lyman-α bulge. This magnetospheric convection pattern is driven by a longitudinal mass asymmetry in the Io plasma torus [Dessler, Sandel, and Atreya, 1981]. Substantial dissociation and ionization of H_2 as well as heating occur in this preferred region of precipitation, but magnetospheric electrons penetrate too deeply for H_2 band emission to escape absorption by overlying CH_4 [Strobel, 1979].

Another ionization source that involves satellites is the electromagnetic interaction of Io with Jupiter. Goldreich and Lynden-Bell [1969] argued that Io is a unipolar generator that develops a potential drop of 400 kV across its radial diameter and drives a current system along its magnetic flux tube. Each foot of the flux tube imbedded in the Jovian ionosphere carries a current of $\sim 10^6$ A principally by keV electrons with power dissipation that can approach 4×10^{10} W [Goldreich and Lynden-Bell, 1969; see also Dessler and Chamberlain, 1979]. The mechanisms for charged-particle acceleration are still uncertain. Ionization and UV radiation constitute part of the power dissipation by energetic charged particles. Atreya et al. [1977] measured localized Lyman-α emission of ~ 300 kR (assumed from a spot with diameter 1000 km) that almost

certainly originated from the foot of Io's flux tube. (A revision by a factor of about 2.6 in the geocoronal Lyman-α calibration factor changes the hot spot Lyman-α intensity reported by Atreya et al. [1977] from 120 to 300 kR.) Based on H_2 cross sections, approximately 10 ion pairs are produced for each Lyman-photon emitted [Cravens, Victor, and Dalgarno, 1975]. Thus at each flux tube foot approximately 3×10^{12} ionization events $cm^{-2}\ s^{-1}$ accompany the observed Lyman-α emission. An alternate explanation of the observed hot spots is a transient manifestation of the interaction between the active sector in the magnetic-anomaly model of the Jovian magnetosphere and the Io plasma torus as a consequence of longitudinal density gradients and current driven plasma instability [Dessler, Sandel, and Atreya, 1981].

During the Voyager encounters with Jupiter, when the Io plasma torus densities were high, the auroral activity occurred over an extensive area of Jupiter's polar region (width ~6000 km), which corresponded to magnetic field lines that map the Io plasma torus into Jupiter's atmosphere, rather than being confined to the Io flux tubes [Broadfoot et al., 1979; Sandel et al., 1979]. The measured intensities were approximately 40 kR of Lyman-α and 80 kR of H_2 Lyman and Werner bands [Broadfoot et al., 1981] and corresponded to an energy deposition rate of ~10–30 ergs $cm^{-2}\ s^{-1}$ or $2–6 \times 10^{13}$ W of 3–30 keV electrons and a column ionization rate of $\sim 1 \times 10^{12}\ cm^{-2}\ s^{-1}$ [Yung et al., 1982]. These large ionization rates are considerably greater than elsewhere on the planet and thus generate locally enhanced electron-number densities and conductivities in the polar regions as compared to the equatorial and midlatitude ionosphere.

2.4. Ion recombination

The principal atomic ion, H^+, recombines radiatively at a rather slow rate of $\sim 3.5 \times 10^{-12}\ cm^3\ s^{-1}$ at low plasma concentrations and room temperature [Bates and Dalgarno, 1962]. Radiative recombination typically exhibits an electron temperature dependence of the form $T_e^{-0.7}$ [Bates and Dalgarno, 1962]. A similar recombination rate is also appropriate for He^+, but is unimportant due to the rapid removal of He^+ by reaction with H_2.

By virtue of the rapid ion–molecule reaction, $H_2^+ + H_2 \rightarrow H_3^+ + H$, H_3^+ recombination acquires a central role in plasma recombination in Jupiter's ionosphere. Leu, Biondi, and Johnsen [1973] have measured an H_3^+ dissociative recombination rate of $(2.3 \pm 0.3) \times 10^{-7}\ (T_e/300)^{-1/2}\ cm^3\ s^{-1}$. At partial pressures of $\sim 10^{-2}$ Torr (1 Torr = 133 Pascal = 1 mm Hg) and low temperatures (~205 K) they obtained a recombination coefficient for the H_5^+ dimer ($H_3^+ \cdot H_2$) of $(3.6 \pm 1.0) \times 10^{-6}\ cm^3\ s^{-1}$. The available evidence for H_2^+ strongly suggests that it can only recombine slowly as a result of unfavorable potential curve crossings in the ground vibrational level [Bates, 1962; see also references in Gross and Rasool, 1964]. A conservative upper limit of $10^{-8}\ cm^3\ s^{-1}$ can be put on this recombination rate.

Hydrocarbon ions play an important role in the lower ionosphere, principally around and below the homopause. Only limited laboratory studies have been performed on these ions. In many instances the identity of the major recombining ion and the products of recombination are not accurately known. The parent gas serves to identify the recombining plasma. For CH_4 a plasma recombination rate of $3.9 \times 10^{-6}\ cm^3\ s^{-1}$ has been measured by Maier and Fessenden [1975] at room temperature, somewhat larger than the Rebbert, Lias, and Ausloos [1973] value of 1.9×10^{-6}. The dominant recombining ions are probably CH_5^+ and $C_2H_5^+$. As the complexity of the heavy hydrocarbon ions increases, the recombination rate increases initially

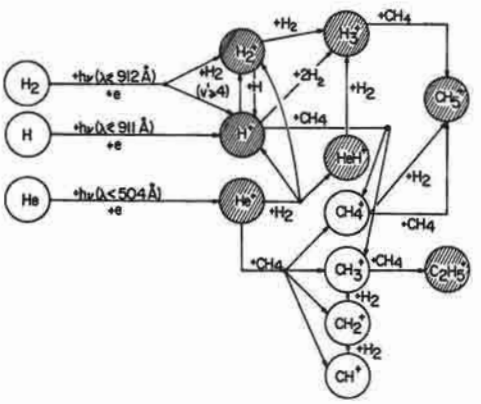

Fig. 2.2. Schematic of the important ionospheric chemical reactions [Atreya and Donahue, 1981]. The hatched circles represent terminal ions that are removed by electron recombination.

(e.g., 5.8×10^{-6} cm^3 s^{-1} for C_3H_8) but eventually it decreases with greater complexity (e.g., 4.2×10^{-6} cm^3 s^{-1} for C_5H_{12} [Maier and Fessenden, 1975]). Unlike hydrocarbon plasmas, recombination in an NH_3 plasma is pressure dependent with a rate varying from 4.6×10^{-6} at 1 Torr to 11.2×10^{-6} cm^3 s^{-1} at 10 Torr [Maier and Fessenden, 1975].

2.5. Ion chemistry

In this section, a brief review of the most important considerations relevant to understanding the ion chemistry of Jupiter is given. A detailed discussion of Jovian ion chemistry is given by Huntress [1974] and Atreya and Donahue [1976], and a recent summary of relevant laboratory data may be found in Huntress [1977]. Important chemical reactions in the Jovian ionosphere are listed in Table 2.1.

The atmosphere of Jupiter consists predominantly of H_2 with $\sim 10\%$ He by volume and trace amounts of CH_4, NH_3, H, and other hydrocarbons. The dominant ion produced at high altitudes by photon and particle impact is H_2^+ (see Fig. 2.1), which quickly reacts with H_2 to form H_3^+ (cf. Table 2.1 and Fig. 2.2). The charge transfer reaction $H_2^+ + H$ is also fast and is important in the topside ionosphere as a H^+ source where $[H] \gtrsim [H_2]$. From the previous discussion, the most important source of H^+ is photodissociative ionization of H_2. Similarly, energetic particles precipitating into the Jovian atmosphere generate secondary electrons that produce considerable H^+ by electron impact dissociative ionization of H_2. An additional source of H^+ is the reaction of $He^+ + H_2$, which is particularly important if He is uniformly mixed with H_2 to very high altitudes. There is appreciable production of He^+ (see Fig. 2.1) and it primarily reacts with H_2 to form H^+ approximately 80% of the time and H_2^+ approximately 20% of the time [Johnsen and Biondi, 1974]. At high altitudes, H^+ does not react with He and $H_2(v)$ unless $v \geq 4$ and thus must either diffuse downward to chemical sinks at lower altitudes or slowly recombine radiatively. These chemical sinks are the reactions

$$\begin{aligned} H^+ + CH_4 &\rightarrow CH_3^+ + H_2 \\ &\rightarrow CH_4^+ + H \end{aligned} \qquad (2.3)$$

$$H^+ + H_2 + H_2 \rightarrow H_3^+ + H_2$$

[Dalgarno, 1971; McElroy, 1973]. During the Voyager encounters with Jupiter, when high thermospheric temperatures were produced by particle precipitation and elevated photoelectron fluxes by high solar activity; photoelectrons with less than 10 eV lose

Table 2.1. *Important reactions in the ionosphere of Jupiter* [Atreya and Donahue, 1976]

Reaction number	Reaction	Rate constant[a]
	Ion production	
*p*1	$H_2 + h\nu \rightarrow H_2^+ + e$	
*p*2	$\rightarrow H^+ + H + e$	
*p*3	$H_2 + e \rightarrow H_2^+ + 2e$	
*p*4	$\rightarrow H^+ + H + 2e$	
*p*5	$H + h\nu \rightarrow H^+ + e$	
*p*6	$H + e \rightarrow H^+ + 2e$	
*p*7	$He + h\nu \rightarrow He^+ + e$	
*p*8	$He + e \rightarrow He^+ + 2e$	
	Ion exchange	
*e*1	$H_2^+ + H_2 \rightarrow H_3^+ + H$	2.1×10^{-9}
*e*2	$H_2^+ + H \rightarrow H^+ + H_2$	$\sim 6.4 \times 10^{-10}$
*e*3	$He^+ + H_2 \rightarrow H_2^+ + He$	$\lesssim 20\%$
*e*4	$\rightarrow HeH^+ + H$ sum	1.0×10^{-13}
*e*5	$\rightarrow H^+ + H + He$	$\gtrsim 80\%$
*e*6	$He^+ + CH_4 \rightarrow CH^+ + H_2 + H + He$	2.4×10^{-10}
*e*7	$\rightarrow CH_2^+ + H_2 + He$	9.3×10^{-10}
*e*8	$\rightarrow CH_3^+ + H + He$	6.0×10^{-11}
*e*9	$\rightarrow CH_4^+ + He$	4.0×10^{-11}
*e*10	$H^+ + H_2 + H_2 \rightarrow H_3^+ + H_2$	3.2×10^{-29}
*e*11	$H^+ + CH_4 \rightarrow CH_3^+ + H_2$	2.3×10^{-9}
*e*12	$\rightarrow CH_4^+ + H$	1.5×10^{-9}
*e*13	$HeH^+ + H_2 \rightarrow H_3^+ + He$	1.85×10^{-9}
*e*14	$H_3^+ + CH_4 \rightarrow CH_5^+ + H_2$	2.4×10^{-9}
*e*15	$CH^+ + H_2 \rightarrow CH_2^+ + H$	1.0×10^{-9}
*e*16	$CH_2^+ + H_2 \rightarrow CH_3^+ + H$	7.2×10^{-10}
*e*17	$CH_3^+ + CH_4 \rightarrow C_2H_5^+ + H_2$	9.6×10^{-10}
*e*18	$CH_4^+ + CH_4 \rightarrow CH_5^+ + CH_3$	1.15×10^{-9}
*e*19	$CH_4^+ + H_2 \rightarrow CH_5^+ + H$	4.1×10^{-10}
	Ion removal/electron–ion recombination	
*r*1	$H_3^+ + e \rightarrow H_2 + H$	see text
*r*2	$H_2^+ + e \rightarrow H + H$	$< 1.0 \times 10^{-8}$
*r*3	$HeH^+ + e \rightarrow He + H$	$\sim 1.0 \times 10^{-8}$
*r*4	$H^+ + e \rightarrow H + h\nu$	see text
*r*5	$He^+ + e \rightarrow He + h\nu$	see text
*r*6	$CH_5^+ + e \rightarrow$ neutral	1.9×10^{-6}
*r*7	$C_2H_5^+ + e \rightarrow$ products	1.9×10^{-6}

[a] The rate constants are in units of $cm^3\ s^{-1}$ for two-body reactions, and $cm^6\ s^{-1}$ for three-body reactions (see Atreya and Donahue [1976] for references).

their energy primarily by vibrational excitation of H_2 [Henry and McElroy, 1969]. Significant departures from a Boltzmann distribution occur at low densities to enhance high vibrational levels. Thus, at high altitudes and low H_2 densities, the reaction

$$H^+ + H_2 (v \geq 4) \rightarrow H_2^+ + H \tag{2.4}$$

is an important loss path for protons [McElroy, 1973; Atreya, Donahue, and Waite, 1979].

Below the homopause or turbopause, the level where an atmosphere ceases to be mixed and where the CH_4 mixing ratio is close to 10^{-3}, He^+ reacts preferentially with CH_4 to yield CH_2^+ and CH^+. Both of these ions react rapidly with H_2 to produce CH_3^+ and CH_2^+, respectively. The ions CH_3^+ and CH_2^+ react quickly with CH_4 to form $C_2H_5^+$ and CH_3^+, respectively. Also CH_4^+ reacts fairly rapidly with H_2 to generate CH_5^+. If CH_4 were the only trace gas in the atmosphere, CH_5^+ and $C_2H_5^+$ would be the terminal ions and would dissociatively recombine to yield CH_4, C_2H_2, and C_2H_4.

In addition to CH_4, there are trace amounts of photochemically produced C_2H_2, C_2H_4, and C_2H_6 in Jupiter's atmosphere [Strobel, 1975; Hanel et al., 1979; Atreya, Donahue, and Festou, 1981]. The ions CH_5^+ and $C_2H_5^+$ are no longer terminal but form other hydrocarbon ions by the following reactions

$$CH_5^+ + C_2H_2 \rightarrow C_3H_5^+ + H_2 \tag{2.5}$$

$$CH_5^+ + C_2H_4 \rightarrow C_2H_5^+ + CH_4 \tag{2.6}$$

[Munson and Field, 1969] and

$$C_2H_5^+ + C_2H_2 \rightarrow C_3H_3^+ + CH_4 \tag{2.7}$$

$$\rightarrow C_4H_5^+ + H$$

$$C_2H_5^+ + C_2H_4 \rightarrow C_3H_5^+ + CH_4 \tag{2.8}$$

$$C_2H_5^+ + C_2H_6 \rightarrow C_4H_9^+ + H_2 \tag{2.9}$$

[Huntress, 1977]. As can be seen, the complexity of ions and possible reactions increase rapidly as additional trace gases are considered. Further insight into hydrocarbon chemistry must await additional laboratory studies and accurate measurements of the hydrocarbon concentrations in the atmosphere.

2.6. Observations of Jupiter's ionospheres

The Pioneer 10 and 11 spacecraft obtained a total of four radio occultation measurements of the Jovian ionosphere. Measurements were made during immersion (latitude 26° N, solar zenith angle, $\chi = 81°$, late afternoon and at latitude 79° S, $\lambda_{III} = 239°$, $\chi = 93°$, early morning), where λ_{III} is System III (1965) longitude, and emersion (latitude 58° N, $\chi = 95°$, early morning and at latitude 20° N, $\lambda_{III} = 91°$, on the evening side) with Pioneer 10 and 11, respectively [Fjeldbo et al., 1975, 1976]. The electron-number density profiles obtained from inversion of the data are shown in Figure 2.3. There are two distinctive features of these profiles. All have large plasma scale heights on the topside (~400–800 km) and exhibit pronounced layered structure on the bottomside. The profiles also reveal a strong possibility of spatial and temporal variations. The assumptions of a topside ionosphere comprised of H^+ and electrons in diffusive equilibrium and thermal equilibrium among the electrons, ions, and neutrals [Henry and McElroy, 1969; Nagy et al., 1976] implies temperatures of 600–900 K.

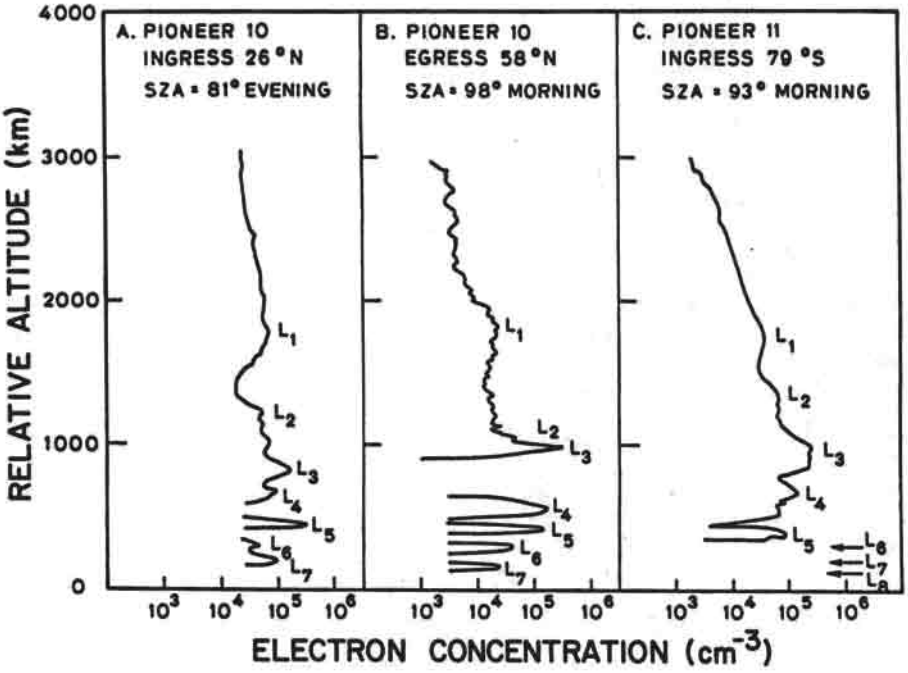

Fig. 2.3. Pioneer 10 and 11 radio occultation measurements of the electron-number density profiles [Fjeldbo et al., 1975]. The Fjeldbo et al. figures have been redrawn on a common height scale by Chen [1981]; the altitude reference is at a density of 10^{19} cm^{-3}, which lies approximately 50 km above the ammonia cloud tops.

The calculations of Nagy et al. [1976] suggest that thermal equilibrium breaks down at an altitude slightly above the peak in electron concentration for high exospheric temperatures. The earlier photoelectron heating calculations of Henry and McElroy [1969] neglected transport effects, although the calculations of photoelectron fluxes and heating rates by Swartz, Reed, and McDonough [1975], Kutcher, Heaps, and Green [1975], and Nagy et al. [1976] took transport effects into account. The two-stream calculations of Nagy et al. [1976] yield a maximum electron heating rate of ~ 50 eV cm^{-3} s^{-1} at an altitude of ~ 450 km above the ammonia cloud tops ($P \simeq 0.6$ bar, $T \approx 150$ K); and a maximum photoelectron escape flux of $\sim 3 \times 10^6$ cm^{-2} s^{-1} at 10 eV.

Although ionospheric scintillations and multipath propagation effects were encountered and in some regions were severe, some bottomside layers are real structure in the ionosphere, e.g., in Figure 2.3a layers L_3 and L_5 [Fjeldbo et al., 1975]. The origin of these layers was attributed to the presence of metallic ions (such as Na^+ from the Io plasma torus) similar to the Earth's sporadic E layers [Atreya, Donahue, and McElroy, 1974] and ionization of CH_3 radicals [Prasad and Tan, 1974]. Chen [1981] has calculated the flux of Na^+ and S^+ to be 3×10^4 cm^{-2} s^{-1} and 4×10^3 cm^{-2} s^{-1}, respectively, in order to produce layer L_6.

The Voyager 1 occultation measurements were made at 12° S, $\lambda_{III} = 63°$, $\chi = 82°$, dip angle $I = 45°$, late afternoon during entry and 1° N, $\lambda_{III} = 314°$, $\chi = 98°$, $I = 16°$, predawn during exit [Eshleman et al., 1979a]. In Figure 2.4 the entry profile has a peak electron-number density of 2.2×10^5 cm^{-3} at 1600 km above the 1 mb level and topside scale heights of 960 and 590 km above and below the 3500 km level,

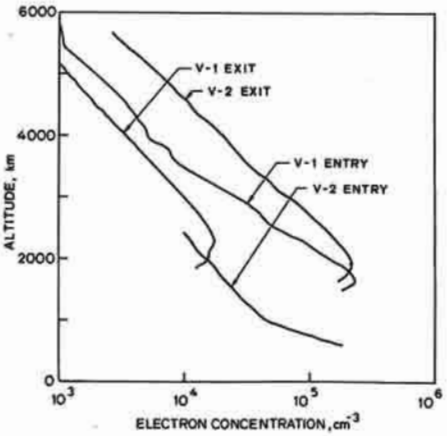

Fig. 2.4. Voyager 1 and 2 measurements of the electron-number density profiles. The geometry of the Voyager 1 measurements is: entry: 12° S, 63° W, solar zenith angle 82°, late afternoon: exit: 1° N, 314° W, solar zenith angle 98°, predawn. The latitude Jovigraphic and the longitude is System III (1965). The Voyager 2 occultations occurred at: entry: 66.7° S, solar zenith angle 87.9°, evening conditions where the ionosphere has been sunlit for hours; exit: 50.1° S, solar zenith angle 92.4°, morning conditions, the lower regions of the ionosphere have just emerged into sunlight after having been in darkness for hours. The zero of the altitude scale corresponds to the 1 mb pressure level that lies approximately 160 km above the ammonia cloud tops (from Eshleman et al. [1979a] and Voyager RSS team).

respectively. The exit profile, where the ionosphere was in darkness for ~5 hours, has a peak electron-number density of 1.8×10^4 cm^{-3} at 2300 km and constant topside scale height of ~960 km. The high altitude of the peak is indicative of an equatorial ionosphere. The poor assumption of protons and electrons in ambipolar diffusive equilibrium across magnetic field lines yields a plasma temperature of approximately 1250 K for the larger scale height [Eshleman et al., 1979a; Atreya, Donahue, and Waite, 1979]. Only if the electron-number density is chemically controlled can an accurate temperature be extracted from the plasma scale height in the equatorial ionosphere. A comparison of the two profiles indicates a net chemical loss rate of $\sim 10^{-4}$ s^{-1} at 2300 km during the night. It should be noted that the entry profile was obtained in the hydrogen Lyman-α bulge region, which has higher H and presumably higher H^+ densities than nonbulge regions [Sandel et al., 1980]. Thus, the chemical loss rate could be smaller than inferred above. The entry profile, being a midlatitude profile, because of its 45° dip angle, implies that the observed change in the electron concentration could be simply a manifestation of an equator to midlatitude variation. An examination of the numerous Pioneer electron concentration profiles, however, reveals no such variation. On the other hand, there is a striking increase in the topside temperature from the Pioneer to the Voyager epoch, making the chemical loss of H^+ via vibrationally excited H_2 ($v' \geq 4$) a viable mechanism during the Voyager observations [Atreya, Donahue, and Waite, 1979]. One should further note that on Saturn where the topside temperatures are relatively low (700-800 K), the peak electron concentration is virtually the same between the equatorial [10° S, Kliore et al., 1980], and high latitude [73° S, Tyler et al., 1981] observations, and no diurnal change was detected. At the low exospheric temperatures prevalent on Saturn, the population of the vibrationally excited H_2 is ignorable, and unless the non-LTE effects are important, the loss of H^+ by charge exchange with H_2 is negligible [Atreya and Waite, 1981].

The Voyager 2 occultation measurements were made at 66.7° S, $\lambda_{III} = 254.8°$, $\chi = 87.9°$, $I = 78°$, evening during entry and 50.1° S, $\lambda_{III} = 148.1°$, $\chi = 92.4°$, $I = 76°$, sunrise during exit [Eshleman et al., 1979b]. The respective plasma scale heights and temperatures are 880 km, 1200 K and 1040 km, 1600 K under the reasonable assumption of ambipolar diffusive equilibrium at midlatitudes [Eshleman et al.,

1979b]. It should be noted that the Voyager 2 entry occurred at a latitude where the Io plasma torus maps into Jupiter's southern polar ionosphere. On exit, a peak electron concentration of $\sim 2 \times 10^5$ cm^{-3} at 2000 km was measured.

2.7. Structure of Jupiter's upper atmosphere

The large plasma scale heights inferred from radio occultation data imply a hot thermosphere because the electrons, ions, and neutrals are approximately in thermal equilibrium [Henry and McElroy, 1969; Nagy et al., 1976]. Similarly, the Voyager ultraviolet solar and stellar occultation data yield large neutral scale heights that indicate a hot thermosphere [Atreya et al., 1979, 1981; Festou et al., 1981]. McElroy [1973] raised the possibility by analogy with the solar corona that upward propagating wave energy could, in principle, create a hot thermosphere on Jupiter. Analysis of the β Scorpii occultation by Jupiter revealed temperature oscillations suggestive of wave propagation in Jupiter's mesosphere [Veverka et al., 1974]. French and Gierasch [1974] evaluated the propagating wave hypothesis and determined that inertia-gravity wave propagation was consistent with the available information. The observed thermal wave amplitudes imply an upward energy flux of ~ 3 erg cm^{-2} s^{-1} and heating rate of ~ 2 K day^{-1}, in considerable excess of the solar EUV flux absorbed above the same level [$\sim 1.3 \times 10^{-2}$ erg cm^{-2} s^{-1}, Strobel and Smith, 1973] and sufficient to account for a hot thermosphere if dissipation of wave energy occurs preferentially within five to ten scale heights above the observed homopause level ($\sim 10^{13}$ cm^{-3}) [Veverka et al., 1974; Atreya and Donahue, 1976; Atreya et al., 1979]. Although the altitude where waves dissipate is not known, the local heating caused by wave dissipation probably results in a steeper temperature gradient than expected for thermal conduction of heat from higher altitudes. This is in contradiction to the oberved temperature (cf., Fig. 2.5).

The same hot thermosphere could also be maintained with less heat input by steady precipitation of soft electrons and protons ($\lesssim 100$ eV) that deposit their energy higher in the atmosphere (~ 0.5 erg cm^{-2} s^{-1} was needed at 10^{11}-10^{12} cm^{-3} density level during the time of Pioneer encounter, [Hunten and Dessler, 1977]; up to ~ 3 erg cm^{-2} s^{-1} at the time of the Voyager encounters [Atreya et al., 1979]). Hunten and Dessler suggested that ionospheric plasma could undergo centrifugal acceleration along flux tubes and be heated by adiabatic compression as a result of flux tube interchange. Based on source strength estimates for ionospheric plasma, they indicated that the heating rate would be deficient by at least one order of magnitude, but noted that plasma associated with Io's torus might supply a sufficient energy flux.

The strong emission of H Lyman-α and H_2 Lyman and Werner bands in the polar and equatorial regions during the Voyager encounter is conclusive evidence for particle precipitation on almost a global basis [Broadfoot et al., 1979; Sandel et al., 1979; McConnell, Sandel, and Broadfoot, 1980]. The energy deposition rate in the auroral regions corresponds to a globally averaged deposition rate of ~ 1 erg cm^{-2} s^{-1}, approximately 80 times the solar heating rate [Yung et al., 1982]. In addition, the 2.8 kR of dayside equatorial H_2 Lyman and Werner band emission requires a particle deposition rate of 0.4 erg cm^{-2} s^{-1} or diurnally averaged rate of ~ 0.2 erg cm^{-2} s^{-1}. These deposition rates are lower than the 3 erg cm^{-2} s^{-1} heating rate inferred by Atreya et al. [1979] from the determination of the Jovian exospheric temperature with the Voyager UVS solar occultation data. However, it is probable that the particle heating is due to softer electrons [Hunten and Dessler, 1977] and occurs higher in the atmosphere than assumed by Atreya et al. [1979]; then only 0.3-0.8 erg cm^{-2} s^{-1} would be required. But this is still an order of magnitude larger than the soft electron deposition inferred from Jupiter's nightside airglow by McConnell, Sandel, and Broadfoot [1980]. It would

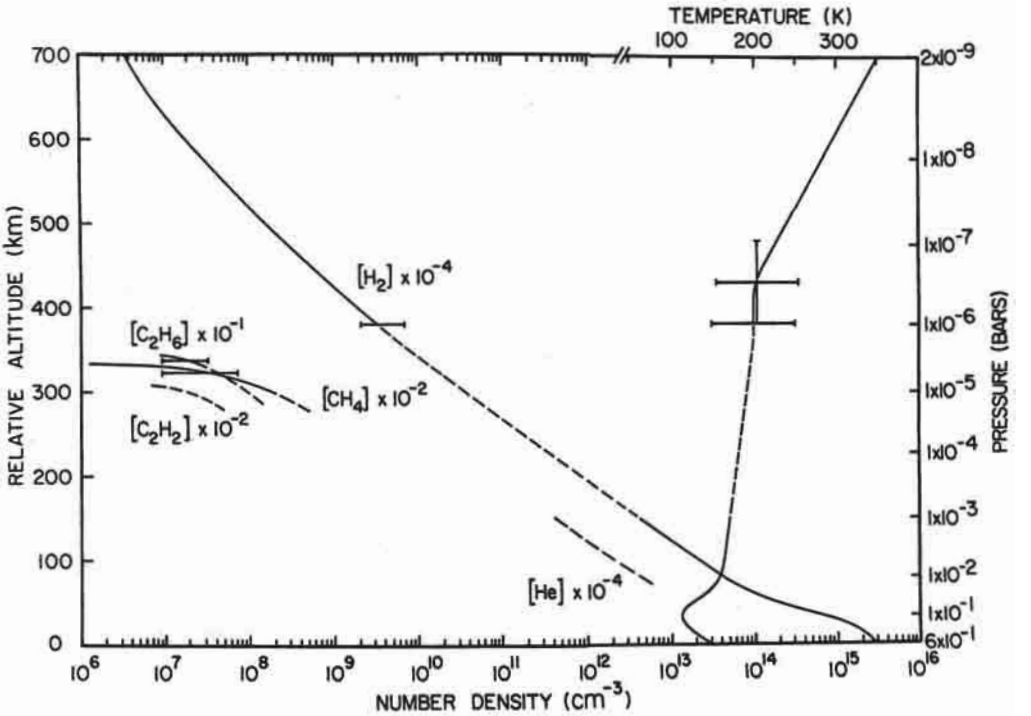

Fig. 2.5. Measured distribution of gases and temperature in the atmosphere of Jupiter [Atreya, Donahue, and Festou, 1981; Festou et al., 1981]. The upper atmospheric data ($z \geq 330$ km) are from Voyager UVS measurements, although the lower atmospheric data are from Voyager IRIS, and RSS experiments.

appear that energy deposition in the auroral regions may be the major source of heat for the thermosphere during periods characteristic of the Voyager encounters.

Of primary importance to ionospheric modeling studies are the distributions of the major gases and temperature at ionospheric heights. The structure of the neutral upper atmosphere has been determined predominantly as a result of the UVS solar and stellar occulation experiments; some significant complementary data have been provided by IRIS (infrared spectrometer) and RSS (radioscience) measurements as well. In a Voyager 1 solar UV occultation experiment, analysis of the continuum absorption by H_2 in the 600-800 A region yielded a neutral temperature of 1450 ± 250 K at 1750 ± 250 km [Atreya et al., 1979]. An alternate analysis of the solar occultation data yields temperatures somewhat lower; however, with the statistical uncertainties of the two analyses considered, the range of deduced temperatures overlap. This temperature is nearly the same as the plasma temperature determined at the same equatorial latitude and at approximately the same time by the RSS experiment [Eshleman et al., 1979a]. The solar occultation experiment did not provide information on the lower thermosphere and mesosphere owing to the large angular diameter of the Sun (0.1°) and the range of the spacecraft (7 R_J). The ultraviolet occultation of a star Regulus (α Leo, HD 87901, B7V, V 1.35) as monitored by Voyager 2 provided temperature and composition profiles above ~330 km altitude measured from the ammonia cloud tops which are located at $P \simeq 0.6$ bar, $T \approx 150$ K. Analysis of these data yielded density profiles of CH_4, C_2H_2, C_2H_6, and H_2, and the temperature profile shown in Figure 2.5

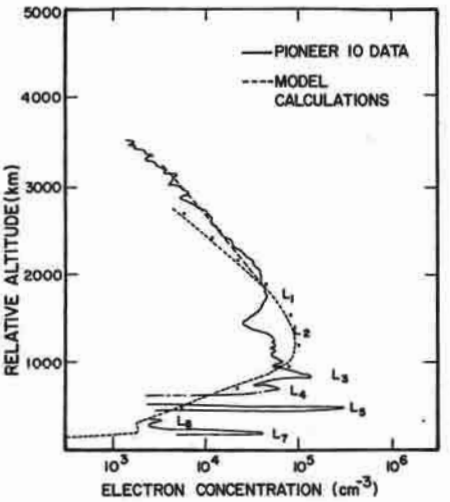

Fig. 2.6. Comparison of electron concentration profile measured by the Pioneer 10 radio occultation experiment (Fig. 2.3b) and model calculations assuming a 1000 K exospheric temperature. The short-dashed curve assumes a $T^{-0.5}$ variation for radiative recombination rate, α_r of H^+ and He^+. Joining of X's will yield the profile when $\alpha_r \propto T^{-0.75}$. The long-dashed curve shows the distribution under the assumptions of diffusive equilibrium, and $\alpha_r \propto T_e^{-0.5}$. The main ion is H^+, except that the secondary peak at the location of layer L_7 is where production of CH_3^+ peaks. The height scale is the same as in Figure 2.3b [Atreya and Donahue, 1976].

[Atreya, Donahue, and Festou, 1981; Festou et al., 1981]. The hydrocarbon mixing ratios were also measured in the stratosphere by IRIS [Hanel et al., 1979], and considerable variability, both temporal and latitudinal, were found in those values. Because the main ionosphere lies far above the region of the hydrocarbons, ionospheric models there are insensitive to the hydrocarbon densities.

2.8. Ionospheric modeling

In this section, the significant points concerning Jovian ionospheric calculations and including attempts at modeling one ionospheric profile measured by the Voyager RSS experiment are presented. Chemical reactions important in the ionosphere of Jupiter are listed in Table 2.1 taken from Atreya and Donahue [1976]. These reactions are illustrated in a flow diagram [Fig. 2.2, Atreya and Donahue, 1981]. In addition to these reactions, the reaction of protons with vibrationally excited H_2 with subsequent removal of the resulting molecular ion by reactions (*e*1) and (*r*1) in Table 2.1 becomes important under conditions of high exospheric temperature [McElroy, 1973; Atreya, Donahue, and Waite, 1979a].

$$(e20)\ H^+ + H_2 (v \gtrsim 4) \rightarrow H_2^+ + H \qquad (2.10)$$

The Pioneer 10 and 11 observations were made near minimum solar activity. The assumption of solar EUV being the principal ionization source in the Jovian atmosphere appears to be adequate for reproducing most of the observed characteristics. Given absorption of solar EUV and associated ionization and the ion atom/molecule interchange and removal in Table 2.1, a set of nonlinear differential equations can be solved numerically to generate a model of the ionosphere. Atreya and Donahue [1976] attempted to calculate the ionospheric profile appropriate to the observation geometry of a Pioneer 10 radio occultation (Fig. 2.3b). They assumed an eddy diffusion coefficient of 2×10^7 cm^2 s^{-1} at the homopause, hydrocarbon density distribution as given by Strobel [1975], and an atmospheric density distribution corresponding to a high exospheric temperature of 1000 K. The results of their calculations for different assumed radiative recombination rates of the terminal ion H^+ and for diffusive equilibrium conditions are shown in Figure 2.6. The main ionospheric distribution is fairly

well reproduced by these model calculations. The layers L_1-L_7 are probably due to sporadic *E*-type clustering of ions such as Na^+ [Atreya, Donahue, and McElroy, 1974], and protons [Atreya and Donahue, 1976]. The source of the former ions could be meteoric in-fall and/or Io. No measurements of the temperature or neutral species in the upper atmosphere of Jupiter were available at the time of the Pioneer observations; therefore, the model of the neutral atmosphere is constrained principally by ionospheric measurements. It should be remarked also that considerable variations in terms of the number and location of the layers, height of the peak, and the plasma scale height were observed in the three successful radio occultation experiments on Pioneers 10 and 11. In general, however, an average peak electron number density of $(1\text{–}3) \times 10^5$ cm^{-3} at 1000-1300 km with an average topside scale height of about 600 km is a good representation of the ionospheric conditions at Pioneer encounter time.

Considerable variations in the ionospheric characteristics were also seen as a function of solar zenith and angle and latitude in both the Pioneer and Voyager observations. The Voyager 1 data (Fig. 2.4) show a dramatic decrease in the peak electron-number density from dayside to nightside. A preliminary attempt at modeling one of the observations, the Voyager 1 entry occultation, is described here. Assuming the photochemical scheme (Table 2.1) applicable for the Pioneer observations, but including the reaction *e*20, which is important for elevated exospheric temperatures [Atreya et al., 1979], Atreya and Donahue [1981] have repeated the calculations with the solar flux (February, 1979 values, H. E. Hinteregger, personal communication) adjusted for the latitude and solar zenith angles of the Voyager 1 entry occultation. The thermal and neutral composition distributions in the atmosphere were taken from the actual observations as opposed to a model as in the Pioneer calculations. The eddy diffusion coefficient at the homopause, K_h, was assumed to be 1×10^6 cm^2 s^{-1} based on the analysis of the equatorial solar and stellar occultation data by Atreya, Donahue, and Festou [1981] and Festou et al. [1981]. The globally averaged value of K_h was also found to be $\sim 10^6$ cm^2 s^{-1} by McConnell et al. [1981], Yung and Strobel [1980], and Broadfoot et al. [1981].

We show in Figure 2.7 the calculated electron concentration density profile taken from Atreya and Donahue [1981], along with the Voyager 1 entry data. The calculation yields H^+ as the major ion in the upper ionosphere, while below 700 km, production of H_3^+ dominates and results in heavier molecules such as $C_nH_m^+$. A comparison between the model and the measurements reveals numerous apparent discrepancies. The following points are noteworthy:

(1) The peak of the measured electron concentration appears greater by about a factor of 3 than the calculated local concentration. We believe that the calculated value is well within the range of uncertainties of the measurements.

(2) The location of the peak in the calculated electron concentration profile appears to be much lower than the measurements. If one believes that the observed maximum at about 1600 km indeed represents the peak in the electron concentration, several possible scenarios for reconciling the calculations with the measurements are possible. First, one could invoke an upward drift of ~ 10 m s^{-1} to raise the peak to the desired height. Aurorally driven thermospheric winds are directed equatorward in a manner similar to the Earth's response to magnetic disturbances [Roble et al., 1979] and induce an upward drift by ion drag. Simple expressions given by Strobel [1970] indicate an equatorward wind of 20 m s^{-1} displaces the electron concentration peak upward by ~ 4 neutral scale heights when $I = 45°$, in reasonable agreement with the height differences in Figure 2.7. Second, if the atomic H number density is equal to or greater than the local H_2 number density in the 1000–2000 km range, a large production of H^+

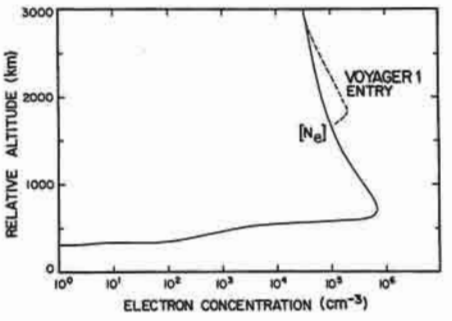

Fig. 2.7. Electron concentration calculated using photochemical scheme described in Table 2.1, and for the geometry of observation corresponding to the Voyager 1 entry occultation (Fig. 2.4). The distribution of gases and temperature in the atmosphere is taken from Figure 2.5 (after Atreya and Donahue [1981]).

by direct ionization of H would result in a completely altered ionospheric structure. This is a distinct possibility because the Voyager 1 entry profile was obtained in the Lyman-α bulge region where atomic hydrogen is probably enhanced [Sandel, Broadfoot, and Strobel, 1980; Clarke et al., 1980; McConnell, Sandel, and Broadfoot, 1981]. On the other hand, it is also likely that the measured maximum in the electron concentration profile does not represent the main ionospheric peak because there may be ionization layers at this altitude or just below giving the appearance of a peak in the electron concentration [Atreya and Donahue, 1981]. This is readily noticeable in the profiles measured by Pioneer 10 and 11 (Figs. 2.3a,b,c). Numerous ionization layers are expected to be present in the atmosphere (V. Eshleman, 1979, personal communication); their analysis, however, is yet incomplete.

(3) The calculated profile shows a slightly greater scale height than the measurements. This is a direct reflection of the assumed exospheric neutral temperture, which is somewhat greater than the plasma temperature. The error analysis of the Voyager RSS data has not yet been completed; it is believed that, within the range of statistical uncertainty, the two temperatures are equal and the scale heights are equivalent.

Although no attempt has been made here to reproduce the equatorial nightside ionosphere, the ideas presented earlier by Atreya, Donahue, and Waite [1979] for the reduction of nighttime electron-number density appear valid. In a relatively hot thermosphere, the conversion of protons to molecular ion H_3^+ takes place with subsequent faster removal of H_3^+ once the ion production source – presumably the Sun – has been turned off (reactions $e20$, $e1$, $r1$). A slow decay of the ionosphere throughout the night is expected. For the electron concentration to drop by a factor of 20 from dayside to nightside, one requires an overall rate constant for the reaction $e20$ to be 4.3×10^{-16} cm^3 s^{-1}. The rate constant for H_2 excited to the fourth vibrational level or higher would have to be $(1\text{–}4) \times 10^{-9}$ cm^3 s^{-1}. Although the rate of this reaction has not been measured in the laboratory, chemical kinetics considerations do not rule out such a value. In addition the vibrational distribution may depart significantly from local thermodynamic equilibrium [McElroy, 1973].

The present attempts to model the measured ionospheric profiles may require improvements, especially if the results of preliminary analysis of the Voyager data remain unaltered after further reduction and analysis of the data. It should be remarked, however, that improved analysis of the data has already begun to give the indication that the measured peak in electron concentration does not represent the actual peak and that the actual peak indeed appears to lie well below 1600 km (R. H. Chen, private communication, 1981) as has been surmised earlier by Atreya and Donahue [1981]. The lack of knowledge of the particle precipitation, including the possible low-energy electron drizzle in the equatorial region, atomic hydrogen distribution, and statistical uncertainties of the dynamics have hampered efforts to carry out realistic calculations.

2.9. Concluding remarks

It would appear on the basis of the Pioneer and Voyager obervations, which occurred at approximately solar minimum and maximum conditions, respectively, that Jupiter's ionosphere and thermosphere undergo significant solar cycle changes. However, the differences between the Pioneer and Voyager encounters may reflect differences in volcanic activity on Io, which ultimately supplies mass to the plasma torus. The Io plasma torus densities appear to be significantly higher during the Voyager encounter period than the Pioneer encounter period [Pilcher and Strobel, 1981; Intriligator and Miller, 1981]. During times of high plasma torus densities, pitch-angle scattering of energetic magnetospheric electrons is enhanced and occurs at lower energies than possible during low-density conditions. Precipitation of energetic electrons is preferentially into Jupiter's polar regions along magnetic field lines connected to the Io plasma torus. Thus, high densities in the plasma torus lead to intense auroral precipitation, which generates significant increases in dissociation and ionization of H_2 as well as intense localizing heating. As a consequence of aurorally driven thermospheric wind systems, atomic hydrogen and heat are redistributed on a global basis and result in an enhanced Lyman-α albedo and elevated temperatures in the thermosphere, in agreement with the differences between the Pioneer and Voyager encounters.

For Pioneer conditions, the ionosphere outside of the auroral zone is produced primarily by solar EUV radiation. The hot thermosphere is maintained either by wave dissipation or soft electron precipitation. Auroral activity appears to be confined to local hot spots that coincide with flux tubes of the Galilean satellites mapped into the atmosphere. Voyager conditions are characterized by an even hotter thermosphere ($\sim$ 400 K warmer), primarily owing to additional particle precipitation. The auroral zones are complete ovals, delineated by strong emissions of H_2 Lyman and Werner bands and H Lyman-α and have enhanced electron concentrations. In the equatorial regions, strong airglow emission from H_2 suggests that particle precipitation may also contribute to the ambient electron concentrations. Because the Voyager 1 entry profile was in the hydrogen bulge region, the initial modeling attempt illustrated in Figure 2.7 does not allow definite conclusions on the relative contributions of solar EUV and precipitating electrons as ionization sources.

Comparison of Pioneer and Voyager electron concentration profiles suggests that Jupiter's ionosphere is at least as complex and variable as the Earth's ionosphere. Of potential importance but still poorly understood is the multilayered structure of Jupiter's ionosphere. The Pedersen conductivity plays a fundamental role in the electrical coupling of the magnetosphere and ionosphere. This quantity, which when divided by the electron number density maximizes at $[H_2] \sim 3 \times 10^{13}$ cm^{-3}, precisely in the layered region of the ionosphere. Note that in Figure 2.6 for Pioneer conditions this is the L_6- L_8 region, whereas for Voyager conditions in Figure 2.7 the main contribution to the Pedersen conductivity occurs in the 300–700 km region where no RSS measurements have yet been reduced. Theoretical estimates of the Pedersen conductivity

$$\sigma_{Ped} = \frac{n_e e}{B} \frac{\nu_{in} f_{ci}}{\nu_{in}^2 + f_{ci}^2} \tag{2.11}$$

where B is the magnetic field strength ($\sim$8 G), e is charge, ν_{in} is the ion–neutral collision frequency, and f_{ci} is the ion cyclotron frequency, can be given on the basis of previous discussion and Figures 2.5-2.7. The integrated Pedersen conductivity is

$$\Sigma = \int \Sigma_{Ped} dz \simeq (1 \times 10^{-11} \bar{n}_e + 1 \times 10^{-2}) \text{ mho} \tag{2.12}$$

where $\bar{n}_e$ (in m^{-3}) is the average electron-number density over the neutral H_2 concentration region of (1–300) $\times$ 10^{12} cm^{-3}, and the second term represents the upper ionospheric contribution. When the ionosphere is produced solely by solar EUV radiation, $\bar{n}_e \sim 10^9$ m^{-3} and $\Sigma \sim 0.2$ mho. In the presence of sporadic E layers and/or moderate energetic electron precipitation $\bar{n}_e \sim 3 \times 10^{10}$ m^{-3} and $\Sigma \sim 0.3$ mho. In the auroral regions observed by Voyager where intense energetic particle precipitation is present, $\bar{n}_e$ may be as large as 1×10^{12} m^{-3} and $\Sigma = 10$ mho. Thus considerable variability in the Pedersen conductivity is expected in Jupiter's ionosphere, especially in the auroral regions. It should be noted that B varies from 3.3 to 14 G on Jupiter's surface, and B was assumed to be 8 G in these estimates.

The other important ionosphere in Jovian magnetospheric studies is that of Io. A recent excellent review of Io's atmosphere and ionosphere may be found in Kumar and Hunten [1981]. No additional measurements of Io's ionosphere were made by the Voyager spacecraft. The Pioneer 10 radio occultation experiment detected the presence of an ionosphere on Io comparable to the ionospheres observed on Mars and Venus [Kliore et al., 1973, 1975]. On the dayside ($\chi = 81°$) and downstream they inferred a peak electron concentration of $\sim 6 \times 10^4$ cm^{-3} at an altitude of ~ 100 km with a topside plasma scale height of ~ 200 km and total extent of 750 km. On the nightside and upstream the peak electron concentration was $\sim 10^4$ cm^{-3} but at 40 km with an abrupt termination of the ionosphere at ~ 200 km altitude and much smaller plasma scale height. The corresponding neutral SO_2 concentrations at the surface appropriate for these measurements is $\sim 10^{11}$ cm^{-3} [Kumar and Hunten, 1981].

ACKNOWLEDGMENTS

We acknowledge research support provided by grants from the NASA Planetary Atmospheres Program. We thank the Voyager RSS Team for Figure 2.4. Dr. M. Acuña kindly supplied the dip angles for the Voyager radio occultation points.